

CONVECTIVE SCALING OF INTRINSIC THERMO-ACOUSTIC EIGENFREQUENCIES OF A PREMIXED SWIRL COMBUSTOR

Alp Albayrak*, Thomas Steinbacher, Thomas Komarek and Wolfgang Polifke

Technische Universität München
Fakultät für Maschinenwesen
Boltzmannstr. 15, D-85747 Garching, Germany

For velocity sensitive premixed flames, intrinsic thermoacoustic (ITA) feedback results from flow-flame-acoustic interactions as follows: perturbations of velocity upstream of the flame result in modulations of the heat release rate, which in turn generate acoustic waves that travel in the downstream as well as the upstream direction. The latter perturb again the upstream velocity, and thus close the ITA feedback loop. This feedback mechanism exhibits resonance frequencies that are not related to acoustic eigenfrequencies of a combustor and generates – in addition to acoustic modes – so-called ITA modes. In this work spectral distributions of the sound pressure level (SPL) observed in a perfectly premixed, swirl stabilized combustion test rig are analyzed. Various burner configurations and operating points are investigated. Spectral peaks in the SPL data for stable as well as for unstable cases are interpreted with the help of a newly developed simple criterion for the prediction of burner intrinsic ITA modes. This criterion extends the known $-\pi$ measure for the flame transfer function (FTF) by including the burner acoustic. This way, the peaks in the SPL spectra are identified to correspond to either ITA or acoustic modes. It is found that ITA modes are prevalent in this particular combustor. Their frequencies change significantly with the power rating (bulk flow velocity) and the axial position of the swirler, but are insensitive to changes in the length of the combustion chamber. It is argued that the resonance frequencies of the ITA feedback loop are governed by convective time scales. For that reason, they arise at rather low frequencies, which scale with the bulk flow velocity.

INTRODUCTION

Stricter emission regulations, in particular for nitrogen oxides (NO_x), pushed the development of lean premixed prevaporized (LPP) combustion systems. Such combustors, however, are more susceptible to thermo-acoustic instabilities and also promote noise emissions [1, 2]. These self-excited instabilities arise from a feedback between the unsteady heat release of the flame and flow perturbations – in particular acoustic waves – in a combustor. High amplitude pressure and velocity oscillations resulting from such thermo-acoustic instabilities can cause problems ranging from increased noise emissions to severe damage of the complete system.

Thermo-acoustic instabilities are commonly characterized as acoustic eigenmodes of the combustion system driven by heat release fluctuations of the flame [3]. The flame is viewed as a source, which feeds perturbation energy into the acoustic modes. However, Hoeijmakers *et al.* [4, 5] showed recently that velocity sensitive flames can develop thermo-acoustic instabilities even in a fully anechoic environment. This might appear paradoxical, since all acoustic perturbations generated by the flame leave an anechoic domain without reflection; acoustic modes cannot form in such an environment. Polifke and co-workers, however, identified a so-called *intrinsic thermo-acoustic* (ITA) feedback loop between unsteady heat release by the flame and flow fluctuations at an upstream reference position, which does not involve reflecting boundary conditions [6, 7]. Numerical simulation of intrinsic instabilities of laminar premixed flames in a computational domain with non-reflecting boundary conditions confirmed the results of Hoeijmakers *et al.* [8, 9]. Emmert *et al.* [10] argued that

*Address all correspondence to this author. albayrak@fd.mw.tum.de

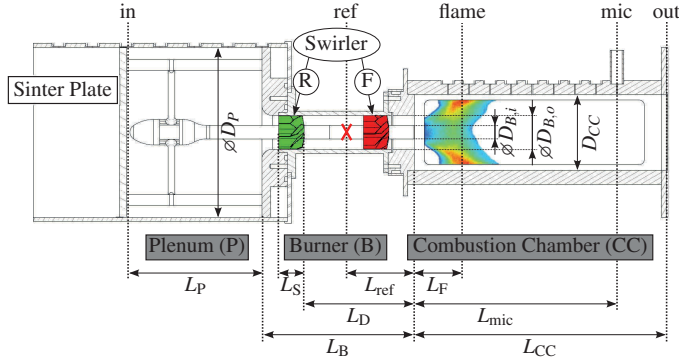


FIGURE 1. SKETCH OF THE BRS TEST RIG.

TABLE 1. PARAMETERS OF THE BRS TEST RIG.

Length	$L_P = 0.17, L_S = 0.03, L_B = 0.18, L_{ref} = 0.07, L_F = 0.045$	
	$L_{CC} = L_{mic} = (0.3, 0.7), L_D = (0.03, 0.13)$	
	$D_P = 0.2, D_{B,o} = 0.04, D_{B,i} = 0.016, D_{CC} = 0.09$ m	
Mean velocity at burner (B)	30, 50, 70 kW	$\bar{u}_B = 11.3, 18.8, 26.4$ m/s
Cross sectional area	$A_P = \frac{\pi}{4} D_P^2, A_B = \frac{\pi}{4} (D_{B,o}^2 - D_{B,i}^2), A_{CC} = D_{CC}^2$	
Temperature	$T_c = 293, T_h = 1930$ K	

close to an odd multiple of $-\pi$ [5, 7, 9]. Furthermore, the gain of the FTF at those frequencies determines if the corresponding ITA mode is stable or unstable: The higher the gain, the more prone the flame becomes to an ITA driven instability. Clearly, a flame may exhibit more than one ITA mode, provided that the gain of the FTF does not decrease rapidly with frequency.

In this work ITA resonances and instabilities of a perfectly premixed, swirl stabilized combustor are investigated, and a refined criterion for the respective frequencies is developed. It is argued that the ITA frequencies depend not only on the phase of the FTF, but also on the acoustic inertia of the burner, plus the ratios of temperature, cross sectional area and specific impedance across the flame. The analysis is validated by experimental results, where (1) the power rating, and thus the mean flow velocity, and (2) the position of the swirler is modified. Although these two measures do not change the acoustic characteristics of the system, significant shifts in peak frequencies of the SPL spectra are observed. These shifts are well predicted by the refined criterion for ITA frequencies.

The measures (1) and (2) both change the gain and in particular the phase of the FTF, i.e. the time scales of the flame response, which are understood to be convective in nature. This suggests that ITA frequencies should exhibit convective scaling. This hypothesis is substantiated by considering how relevant length and velocity scales of a turbulent flame change with the power rating. A simple relation that predicts how resonance frequencies should increase with power rating compares well with experimental results.

This paper is structured as follows: We first describe the experimental setup investigated in this study. Then measurement methods and results for the SPL spectra and the flame frequency response are presented. Subsequently, the distributed time lag model for the FTF is outlined. This is followed by the derivation of an extended criterion for ITA eigenfrequencies, which is then employed to interpret the results. Then convective scaling of the ITA modes is established, the relation to previous studies on lock-on phenomena and entropy modes is outlined.

EXPERIMENTAL SETUP

Measurements presented in this paper were performed on a swirl stabilized, perfectly premixed combustor as sketched in Fig. 1. All parameters are specified in Tab. 1. This setup is known

the ITA feedback should play an important role even for realistic combustor configurations with (partially) reflecting boundaries, because ITA modes exist in addition to acoustic cavity modes and can for certain conditions be dominantly unstable. Results of Mukherjee et al. support these findings [11]. It is particularly interesting that the standard methods for passive control of thermoacoustic instabilities (i.e. acoustic liners and decreasing boundary reflection coefficients) may not stabilize ITA modes. As shown by Emmert *et al.* [10], just the opposite effect can be observed, i.e. increased acoustic losses at the combustor exit can enhance the ITA feedback and lead to increased growth rates. Silva et al. [12] showed that ITA resonances can lead to the formation of characteristic peaks in the spectral distribution of the sound pressure level (SPL) of broad-band combustion noise of turbulent flames.

Fundamentally, an ITA feedback exists because the sound emitted by an unsteady flame *directly* – i.e. without reflection of acoustic waves by the environment – disturbs the velocity field in the vicinity of the flame. This argument is developed in more detail as follows: Premixed flames respond to perturbations of upstream velocity with a change in their heat release rate. This, in turn, generates acoustic waves which travel in both upstream and downstream direction. The upstream propagating acoustic waves perturb the upstream velocity and, thus, close a feedback loop. It has to be stressed out again, that such intrinsic modes can exist in addition to the acoustic modes (‘cavity modes’). The described intrinsic feedback loop is affected but not eliminated by acoustic reflections at the boundaries or area jumps. Therefore, the contribution of the ITA feedback needs not to be close to acoustic eigenfrequencies of the combustor although it might interact with them.

The characteristics of the ITA modes are largely determined by the flame transfer function (FTF), which relates velocity fluctuations u'_{ref} at a reference position – usually close to the flame anchoring position – to fluctuations of the heat release rate \dot{Q}' . In previous studies it was argued that the frequencies of the ITA modes coincide with frequencies where the phase of the FTF is

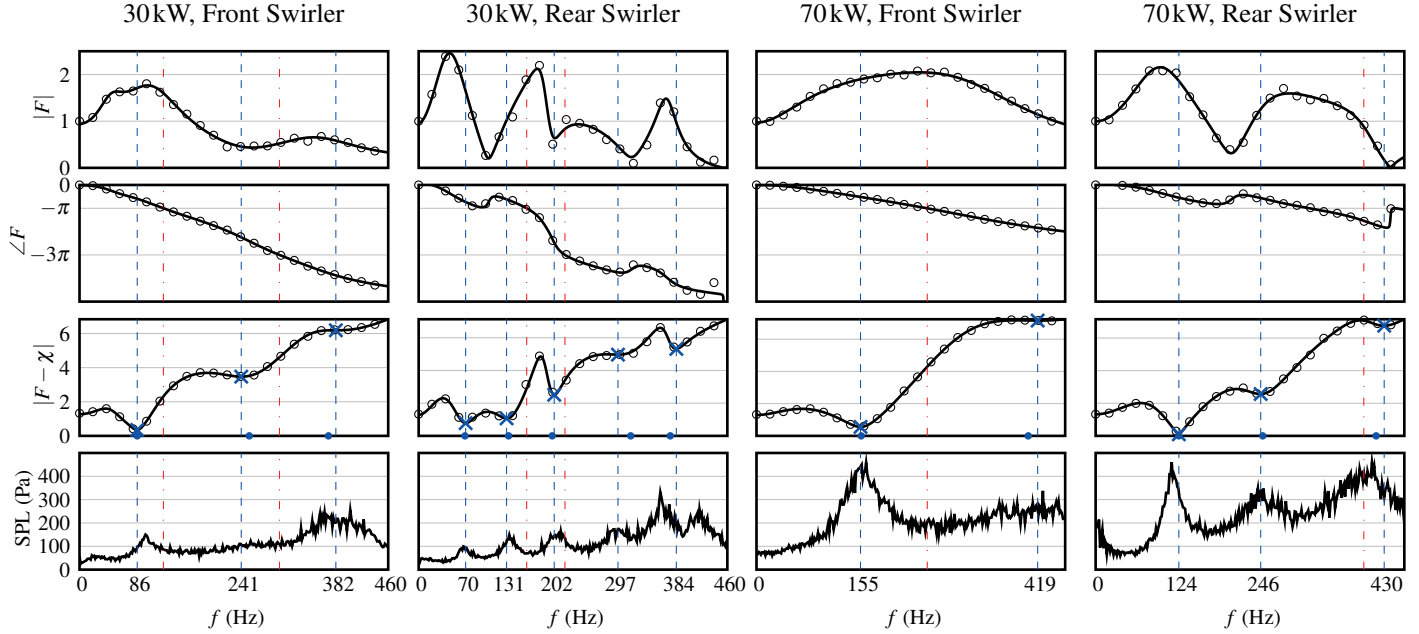


FIGURE 2. ROW 1 AND 2: GAIN AND PHASE OF FFR and FTF. ROW 3: ABSOLUTE VALUE OF DISPERSION RELATION. ROW 4: MEASUREMENTS OF SOUND PRESSURE LEVELS. FOR FIRST THREE ROWS: MEASUREMENTS \circ , MODEL —. \bullet SOLUTION OF $F_M - \chi = 0$. \times LOCAL MINIMA OF $|F - \chi|$. VERTICAL LINES: $-(2n + \pi)$ CRITERION - - -, EXTENDED CRITERION - - -.

as the ‘BRS burner’ and has served as a base for several numerical and experimental studies, e.g. [13–15]. It consists of a cylindrical plenum (P) with an inner diameter of D_P and a length of L_P . A sinter plate is placed at the upstream end of the plenum. The porous material allows flow to pass through, but at the same time provides a defined acoustic hard wall boundary condition. The sinter plate is axially movable, which allows to force the flame over a wide range of frequencies with significant amplitude [16]. At the combustor exit a perforated plate is employed in order to achieve a boundary condition with reduced acoustic reflections.

Attached to the plenum is the burner (B) which is an annulus with an inner diameter of $D_{B,i}$ and an outer of $D_{B,o}$. A swirler mounted on a central bluff body can be placed at two axial positions denoted by ‘R’ for the rear and ‘F’ for the front position. The front position is located at 30 mm before the combustion chamber, the rear at 130 mm. A change in the swirler positions results in a significant change of the flame frequency response (FFR). Inspired by studies of Straub and Richards [17] on the effect of fuel nozzle configuration on premix combustion dynamics, this effect was explained by Komarek and Polifke [13] with the superposition characteristic of acoustic and swirl related (convective) time lags. Since the acoustic time scale is small compared to the convective one, a change in the swirler position by half a convective wavelength alters the superposition of the individual contributions significantly. The swirler with

an axial length L_S has eight vanes, which turn the flow by approximately 45° . This leads to a swirl number of approximately 0.74. The combustion chamber (CC) has a square cross section and a variable axial length L_{CC} . Two settings were considered: One where this length is fixed to $L_{CC} = 300$ mm and one with $L_{CC} = 700$ mm. For a power rating of 30 kW the first leads to a stable operating point, while the latter is unstable.

The combustor is operated with a methane-air mixture at an equivalence ratio of $\bar{\phi} = 0.77$ with three power settings 30, 50 and 70 kW. Each corresponds to a bulk axial flow speed inside the burner annulus \bar{u}_B which increases with the power ($\bar{u}_B = 11.3, 18.8$ and 26.4 m/s). This leads to a small axial shift of the maximum of the flame’s heat release and, thus, to a slight elongation of the flame. The swirler position only has a negligible effect on the heat release distribution [13].

Spectral Distribution of SPLs

Time series of pressure fluctuations are measured by a microphone placed at the position ‘mic’ in Fig. 1. From these data the noise level in terms of the SPL spectrum is estimated using Welch’s method with a symmetric Hamming window of a width of 20000. No acoustic excitation was applied here.

The SPL results for the 30 kW and 70 kW cases with a short combustion chamber with $L_{CC} = 300$ mm are plotted in the last row of Fig. 2. These cases correspond to a stable operating condi-

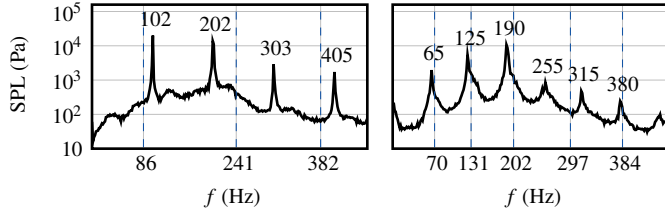


FIGURE 3. THE SOUND PRESSURE LEVELS FOR UNSTABLE 30 kW CASE. LEFT/RIGHT: FRONT/REAR SWIRLER POSITION. VERTICAL LINES: EXTENDED CRITERIA - - -

tion. Accordingly, the SPL spectra show several fairly broad resonant peaks. Fig. 2 shows clearly that under variation of power rating or swirler position both frequencies and amplitudes of the peaks change. These changes in frequency are remarkable, because the speed of sound in the plenum and combustor, which governs the acoustic eigenfrequencies of the test rig, is not affected by changes in the power rating or swirler position.

By increasing the combustion chamber length from $L_{CC} = 300$ mm to $L_{CC} = 700$ mm, the 30 kW cases becomes unstable. Fig. 3 shows the corresponding noise spectrum. The front position case (left plot) has a strong peak at a frequency near 100 Hz and its multiples. Similarly, the rear position case (right plot) has a peak frequency near 60 Hz and its multiples. For the 70 kW power rating with the elongated combustion chamber the combustor is stable, therefore the SPL spectrum is not shown here.

MEASUREMENT OF FLAME FREQUENCY RESPONSE

The flame frequency response (FFR), which describes the response of the flame to upstream velocity perturbations, is determined by acoustically exciting the flame with a siren [16]. The normalized axial velocity fluctuations $u'_{\text{ref}}/\bar{u}_{\text{ref}}$ at a point 70 mm upstream of the beginning of the combustion chamber (marked by a cross in Fig. 1) are related to the normalized integrated heat release fluctuations Q'/\bar{Q} of the flame at discrete frequencies ω_n :

$$F(\omega_n) = \frac{Q'(\omega_n)/\bar{Q}}{u'_{\text{ref}}(\omega_n)/\bar{u}_{\text{ref}}}, \omega_n \in \mathbb{R}. \quad (1)$$

The velocity signal was captured by a CTA probe and the heat release by a photomultiplier with an interference filter attached (centered on a wavelength of $307.1 + 3/-0$ nm; half power bandwidth of 10 ± 2 nm; transmission of 15%).

For the stable configuration with a short combustion chamber $L_{CC} = 300$, the FTF was measured for two power ratings 30 and 70 kW, each with the swirler mounted in the front and the rear position, respectively. The results are again shown in Fig. 2 (◊ symbol). For the front swirler position (left plots), the transfer function has for both power ratings a single excess of gain at low

frequencies, followed by a smooth decay, while the phase can be approximated with a constant negative slope.

For swirler mounted in the rear position the gain of the FFR exhibits pronounced maxima and minima, which can be explained as the effect of constructive and destructive superposition of several contributions with different time lags. As mentioned in the introduction, the flame response of a swirl flame includes contributions from acoustic and swirl waves [13, 18]. The difference in time lags is significantly larger for the rear swirler position, which leads to more frequent extrema in gain due to alternations between constructive and destructive interference (see Blumenthal *et al.* [19]). For the swirler mounted in the rear position, the phase follows the same overall slope as for the front position, but is distorted at several frequencies, i.e at 100 Hz for the 30 kW and at 210 Hz for the 70 kW cases. The distorted frequencies match with the local minima of the gain. This is a typical behavior of systems which are governed by processes with different time scales, c.f. [20] for an illustrative example.

The increase of the power rating from 30 to 70 kW affects noticeably the slope of the phase, since the characteristic time delay of the flame changes. This is largely an effect of the change in the flow velocity \bar{u}_B and the flame length, as described by Alemela *et al.* [21]. This is discussed in more detail below.

MODELING OF FLAME TRANSFER FUNCTION

As suggested by Subramanian *et al.* [22] a distributed time lag model in the form of a stable rational function is used in this work to model the flame transfer function:

$$F_M(\omega) = \sum_{k=1}^n \frac{C_k}{i\omega - A_k}, \omega \in \mathbb{C}, \quad (2)$$

where approximately $n \approx 10$ poles suffice to provide a good fit to the measured flame transfer functions. Here, ω is the angular frequency and i the complex unit. During regression all parameters C_k and A_k are optimized such that the quadratic error between the measured data and the model is minimized. According to Polifke and Lawn [23], the frequency response at the low-frequency limit $\omega = 0$ should be 1, which corresponds to a gain value of 1 and a phase value of 0. By adding these two data points to the experimental data set, we ensure that the resulting FTF satisfies these conditions.

The Bode plot of the resulting FTF for the 30 kW is shown with the solid line — in Fig. 2 (first two columns and first two rows). Similarly, for the 70 kW case the corresponding FTF is shown in Fig. 2 (last two columns and first two rows). Clearly, the fitted models are in excellent agreement with the measurements of the FFR. At frequencies higher than the plotted ones, the model predicts a quick decay of the gain to 0. This agrees well with the low-pass filter behavior of a realistic flame transfer

以上内容仅为本文档的试下载部分，为可阅读页数的一半内容。如要下载或阅读全文，请访问：<https://d.book118.com/065020213003011311>